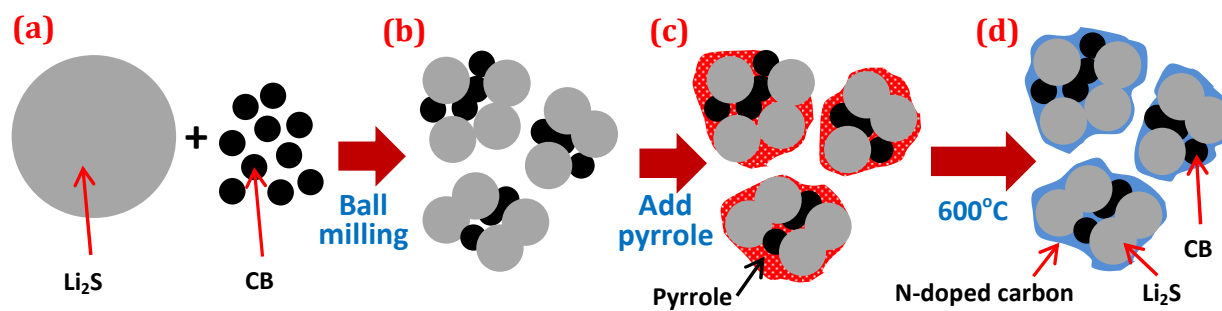


Graphical Abstract



The procedure for the synthesis of $\text{Li}_2\text{S}/\text{C}$ composite particles encapsulated by a nitrogen-doped carbon shell, which exhibit the highest initial discharge specific capacity ever reported in the literature.

Submitted to *Journal of Materials Chemistry A*, August 2014

Li₂S Encapsulated by Nitrogen-Doped Carbon for Lithium Sulfur Batteries

Lin Chen^{a,b}, Yuzi Liu^c, Maziar Ashuri^{a,b}, Caihong Liu^{a,b} and Leon L. Shaw^{a,b,*}

^a Wanger Institute for Sustainable Energy Research

^b Department of Mechanical, Materials and Aerospace Engineering
Illinois Institute of Technology, Illinois, USA

^c Center for Nanoscale Materials

Argonne National Laboratory, Illinois, USA

Abstract

Using high-energy ball milling of the Li₂S plus carbon black mixture followed by carbonization of pyrrole, we have established a facile approach to synthesize Li₂S-plus-C composite particles of average size ~400 nm, encapsulated by a nitrogen-doped carbon shell. Such an engineered core-shell structure exhibits an ultrahigh initial discharge specific capacity (1,029 mAh/g), reaching 88% of the theoretical capacity (1,166 mAh/g of Li₂S) and thus offering the highest utilization of Li₂S in the cathode among all of the reported works for the encapsulated Li₂S cathodes. This Li₂S/C composite core with a nitrogen-doped carbon shell can still retain 652 mAh/g after prolonged 100 cycles. **These superior properties are attributed to the nitrogen-doped carbon shell that can improve the conductivity to enhance the utilization of Li₂S in the cathode.** Fine particle sizes and the presence of carbon black within the Li₂S core may also play a role in high utilization of Li₂S in the cathode.

* Corresponding author: **Leon L. Shaw** (lshaw2@iit.edu)

Introduction

High power and high energy density rechargeable batteries with long cycle life are in urgent demand for electric vehicles and large-scale energy storage devices.¹⁻⁵ Unfortunately, the state-of-the-art Li-ion batteries (LIBs), which have dominated the market for portable electronics, have fallen short for these emerging applications.⁶ To increase the energy density of rechargeable batteries, one of the active areas of research is to develop anode and cathode materials with high specific capacities.¹⁻¹⁰ In this regard, sulfur-based cathodes are considered as one of the strongest cathode candidates for next generation high capacity LIBs.^{11, 12} Sulfur has a theoretical capacity of 1,673 mA h/g, and when coupled with a Li anode, the theoretical specific energy of the lithium-sulfur (Li-S) cell is ~2,600 Wh/kg,^{13, 14} five times higher than that of the commercial LiCoO₂/graphite batteries. Sulfur also offers other advantages, such as low cost, naturally high abundance and non-toxicity.¹⁵ However, sulfur cathodes suffer from three key deficiencies: (i) large volume change of sulfur (~80%) during cycling, (ii) dissolution of long chain lithium polysulfide products (Li₂S_x, 4 < x ≤ 8)¹⁶ into the electrolyte, and (iii) being an ionic and electronic insulator. Extensive progress of sulfur cathodes, including imbedding particles to porous hosts,¹⁷⁻²⁰ coating sulfur within carbon nanotubes^{21, 22} or graphene,²³ and adding additives to trap polysulfides,²⁴ has been made to improve the cycling performance of the cells, but the intrinsic safety hazard when coupled with lithium metal is still remaining.

Li₂S is a promising cathode material due to the ability to be paired with lithium-free anodes (such as silicon and tin), readily alleviating the safety issues.²⁵ Moreover, Li₂S as the final discharge products would experience the initial process of becoming sulfur during delithiation with a volume shrink, and thus volume expansion to cause structure fracture does not exist. However, Li₂S is also an insulator and has the same tricky problem of polysulfides dissolution as S does. Much effort to address these challenges has been pursued, such as hosting Li₂S in microporous carbon²⁶ and coating Li₂S with a conductive polymer²⁷ or carbon.^{6, 28, 29} Despite these advances, good conductivity and superior electrochemical performance of Li₂S cathodes with high ratio of active materials (>70%) have not been

simultaneously realized yet.

Herein, we design a facile technique to prepare the nitrogen-doped, carbon-encapsulated Li_2S with active materials ratio mass as high as 72%. The nitrogen-doped carbon shell can greatly improve the conductivity while simultaneously enabling the effective confinement of polysulfides within the conductive shell. As a result, the cells with the nitrogen-doped, carbon-encapsulated Li_2S as the cathode exhibit an extremely high initial discharge capacity (as high as 1,029 mA h/g). To the best of our knowledge, this specific capacity is the highest among all of the reported works for the encapsulated Li_2S cathodes.^{6, 27-29} This is also the first time that such good structured Li_2S with a high mass ratio achieving excellent cycling performance and superior capacity retention has been reported.

Our approach is schematically displayed in Figure 1. Li_2S particles were first ball milled with carbon black (CB) for 6 hours and then pyrrole was added to the ball-milled $\text{Li}_2\text{S}/\text{C}$ mixture with stirring to yield uniform and intimate contact between the particles and pyrrole. After carbonization of the pyrrole in an Ar atmosphere for 8 hours, the as-prepared samples were collected. The Li_2S -plus-C composite core encapsulated with a nitrogen-doped carbon shell (termed as the carbon coated Li_2S hereafter) was achieved by this route. **This unique Li_2S core shell structure can improve the conductivity, thereby leading to the extremely high initial discharge capacity and high capacities even after prolonged cycling.** The details of our experimental procedures and results are described below.

Experimental

Preparation of ball milled Li_2S : 1 g commercial Li_2S powders (Sigma-Aldrich) were weighed and mixed with 0.075 g CB and 20 g iron balls (different sizes) in a ball milling container within a glove box (MBRAUN), which is maintained with moisture level lower than 0.1 ppm and oxygen level lower than 1 ppm. After sealing the container tightly, the materials were ball-milled for 6 hours in a SPEX machine (SPEX Mixer 8000M).

Subsequently, the tightly sealed container was put back to the glovebox and the materials were collected and termed as “ball milled Li_2S ” for future use.

Synthesis of nitrogen-doped, carbon-encapsulated Li_2S : To prepare the carbon coated Li_2S , 15 droplets of pyrrole (Alfa Aesar) were added to 0.5g of the ball milled $\text{Li}_2\text{S}/\text{C}$ powder in an aluminum oxide crucible. The mixture was stirred for a while to make uniform and intimate contact between the powder and pyrrole. After being sealed within a stainless steel autoclave with a copper gasket inside the glovebox, it was transferred to a furnace for carbonization of pyrrole at 600 °C for 8 hours. After the autoclave was cooled down, it was put back into the glovebox and the materials were collected and marked as “carbon coated Li_2S ”. The quantity of Li_2S in the carbon coated Li_2S was estimated via weight measurement before and after carbonization of pyrrole, and found to be 72 wt% (including the CB in the ball milling step in the calculation).

Characterization: The XRD data were collected in the 2-theta range from 10-100 degree using Bruker X2 with $\text{CuK}\alpha$ radiation. High resolution imaging was conducted with field emission scanning electron microscope (JEOL) in Center for Nanoscale Materials (CNM) at Argonne National Laboratory. EFTEM elemental mapping was obtained with Gatan vacuum transfer holder for protecting Li_2S samples in field emission transmission electron microscopy (JEOL) at CNM. XPS experiments were performed with a Kratos Axis-165 XPS instrument equipped with an Al source (1486.6 eV). Survey and high resolution scans were conducted using pass energy of 80 eV and 20 eV, respectively. Both XPS and EFTEM samples were not exposed to air during loading into the instrument because the sample transfer from the glovebox to the XPS and EFTEM instruments were assisted with an air sensitive transfer holder and Gatan vacuum transfer holder, respectively.

Electrochemical measurements: The carbon coated Li_2S powder was mixed with PVDF and CB (8:1:1 mass ratio) in an Ar-filled glovebox to prepare electrodes with an aluminum foil as the current collector, and the mass loading of active materials for the assembled cells is ~1

mg cm⁻². The electrolyte contained 1 M lithium bis(trifluoromethanesulfonyl)imide (LiTFSI) salt in the dimethoxyethane (DME) and 1,3-dioxolane (DOL) solvents (1:1 v/v) with the LiNO₃ additive (1 wt%). The carbon coated Li₂S cathodes coupled against a lithium metal anode were fabricated in CR2032 coin cells in the glovebox. Cyclic voltammetry (CV) data were achieved using Parstat 4000 (Princeton Applied Research) with a coin cell initially charged from the open circuit voltage to 4.0 V and then the voltage is switched between 1.6 and 3.4 V at a scan rate of 0.025 mV s⁻¹. Electrochemical impedance spectroscopy (EIS) data were also collected with this instrument in the frequency range of 1 MHz to 0.1 Hz **upon the discharge state of batteries**. The cycling performances were evaluated using Arbin System 2000. All charge-discharge processes were started with a slow charge rate of 0.05 C to 4 V and then cycled between 1.6 and 3.4 V at the desired C-rate.

Results and Discussion

Figure 2 shows the X-ray diffraction (XRD) patterns of Li₂S based samples. Since we sealed Li₂S samples in capillary tubes to protect these particles from air during the XRD data acquisition, the pattern of capillary tubes forms the background. Only Li₂S pattern (JCPDS Card No. 26-1188) was observed in both ball milled Li₂S and carbon coated Li₂S,²⁸ suggesting the amorphous carbon in the samples and no side reactions during the preparation process.

The sizes and morphologies of the carbon coated Li₂S were measured using field emission scanning electron microscopy (FESEM). As shown in Figure 3, it can be seen that the sizes and morphologies of carbon coated Li₂S particles are uniform although some agglomerations are also observed. The sizes of particles range from 300 nm to 1.5 μm with the majority at ~400 nm. This is the first time that such small Li₂S particles have been obtained through the ball milling method. Such small particles can effectively reduce the distance for Li ion migration and electron transfer, thereby improving the kinetics of electrochemical reactions in batteries and allowing most of the Li₂S in the cathode to contribute to the specific

capacity.

The core-shell structure of the carbon coated Li_2S was confirmed with energy-filtered transmission electron microscopy (EFTEM) with a Gatan vacuum transfer holder for loading the samples. EFTEM elemental mappings of a carbon-coated Li_2S particle, including carbon, sulfur and nitrogen, are illustrated in Figure 4a, 4b and 4c, respectively. The bright contrast in these images indicates the positions of corresponding element in the particle. This single particle has a size slightly less than 400 nm, consistent with the SEM observation showing that most particles are around 400 nm. Figure 4d is a combination of the elemental mappings where blue, red and green represent carbon, sulfur and lithium, respectively. This EFTEM elemental map unambiguously reveals that sulfur and lithium elements are encapsulated by a carbon shell, demonstrating an excellent core-shell structure. This conclusion is in good accordance with Figure 4a which also displays the presence of a significantly higher carbon concentration at the outer perimeter of the particle than in the interior.

It should be noted that Figure 4a and 4d also reveal the presence of carbon in the interior of the particle. This is not a surprise because the mapping shown in Figure 4 is the projection of a three-dimensional particle, and thus the carbon coating on the surface of the Li_2S particle will result in the appearance of the presence of carbon inside the particle. However, if this is the case, then the carbon distribution within the particle should be uniform and the carbon signal should be significantly weaker than that at the outer perimeter. Clearly, this is not the case because the carbon signal is very strong in some inner regions. We attribute the presence of carbon in some inner regions to the 7 wt% CB (~4.5 vol%) added during ball milling. Therefore, the Li_2S core in this study is, in fact, a Li_2S -plus-C ($\text{Li}_2\text{S}/\text{C}$) composite core. To the best of our knowledge, this is the first time that such $\text{Li}_2\text{S}/\text{C}$ composite cores with an average size ~400 nm are synthesized.

The formation of $\text{Li}_2\text{S}/\text{C}$ composite cores is consistent with the nature of the high-energy ball milling process. It is well established that high-energy ball milling entails repeated fracture

and cold welding of fine particles.^{30,31} Furthermore, when ball milling a two-material mixture with one material having large particle sizes and the other smaller particle sizes, the material with smaller particles are often occluded by the material with larger particles.^{32,33} The CB used in this study is extremely fine, ranging from 20 to 130 nm with majority between 20 and 50 nm (Figure 5). In contrast, the Li_2S powder is coarse ($> 1,000$ nm) before ball milling. Thus, repeated fracture and cold welding of large Li_2S particles during high-energy ball milling could result in occlusion of ultrafine CB, leading to the formation of $\text{Li}_2\text{S}/\text{C}$ composite particles as shown schematically in Figure 1(b). The CB inside the composite particles could form some conductive networks to enhance the utilization of Li_2S in electrochemical reactions.

It is interesting to note that Figure 4c indicates a uniform distribution of nitrogen. This is in a sharp contrast to the carbon mapping which displays strong carbon signals at the outer perimeter along with presence of some carbon inside the particle. This is a bit surprise to us because a previous study³⁴ has shown that the nitrogen atoms from pyrrole are present as a dopant in the carbon coating formed during the carbonization of pyrrole. The nitrogen mapping of Figure 4c, in contrast, may indicate the nitrogen doping of the $\text{Li}_2\text{S}/\text{C}$ composite core. Additional studies are needed in the future to confirm this. For now, it can be concluded that $\text{Li}_2\text{S}/\text{C}$ composite particles are encapsulated by a nitrogen-doped carbon shell, as evidenced by the EFTEM images. **Nitrogen doped carbon has a higher electronic conductivity than carbon without nitrogen doping,**^{34,35} and thus it can greatly enhance the electronic conductivity of the electrode material, enabling fast charge transfer rates.

Analysis of X-ray photoelectron spectroscopy (XPS) was also performed to investigate the nature of nitrogen in the carbon coated Li_2S . The peaks of high resolution XPS spectra of N1s for the carbon coated sample can be clearly seen in Figure 6, demonstrating the presence of nitrogen in the coating layer. After curve fitting, the peaks at 398.5 eV and 400.5 eV can be attributed to nitrogen in C-N and C=N, respectively.^{36,37} The C-N, also called pyridinic-N, means that every nitrogen atom is bonded to two carbon atoms and contribute the aromatic π

system with one p-electron. The C=N, named pyrrolic-N as well, refers that nitrogen atoms bond to two carbon atoms and donate two p-electrons to the aromatic π system.³⁸ These results prove that the carbon coating is doped with nitrogen, in good accordance with the analysis of EFTEM.

The electrochemical performance of the carbon coated Li₂S was evaluated with CR2032 coin cells. The EIS data of Li₂S based batteries **at the discharge state**, shown in Figure 7a, reveals a semicircle in the high frequency range, which is assigned to the charge transfer resistance (R_{ct}).⁸ The carbon coated Li₂S battery has a smaller semicircle compared to that of the ball milled Li₂S battery, indicating the decreased charge transfer resistance due to the improved electronic and ionic conductivities enabled by the nitrogen-doped carbon coating.

In order to further analyze the effect of the nitrogen-doped carbon shell on the electrochemical performance of the electrode materials, CV tests were performed. The CV curves of uncoated and coated Li₂S batteries were compared in Figure 7b and 7c. Based on the report by Yang et al.,³⁹ we used 4 V as the cutoff voltage in the first scan to activate Li₂S, while the remaining cycles were scanned between 1.6 and 3.4 V. **Overall, the CV profiles of two cells look similar, but with some subtle differences. Both cells show three peaks in the first anodic scan. However, in the subsequent anodic scans the three anodic peaks shift to lower potentials and merge into a broad anodic peak the peak position of which is located at 2.45 V for both the carbon coated and uncoated cells. Furthermore, the carbon coated cell also displays a shoulder peak at 2.35 V, whereas this shoulder peak is not obvious in the uncoated cell. For the cathodic scans both cells exhibit two major cathodic peaks at around 2.3 and 2.0 V after the initial scan.** These two cathodic peaks are related to the change from elemental sulfur to higher-order lithium polysulfides (Li₂S_x, $x > 4$) and the reduction of higher-order polysulfides to lower-order polysulfides (Li₂S_x, $x \leq 4$), respectively. The anodic peak at 2.45 V corresponds to the conversion from lower-order polysulfides to higher-order polysulfides and then to elemental sulfur. However, the fact that the uncoated cell does not have an obvious shoulder peak at 2.35 V suggests that the conversion from lower-order

polysulfides to higher-order polysulfides is less active in the uncoated cell than that in the coated cell. Another important difference between the two cells is that all the peak currents in the coated cell are higher than those in the uncoated cell, indicating the increased ion and electron transport enabled by the nitrogen-doped carbon coating.

The galvanostatic charge-discharge tests of coin cells with the coated Li_2S -based cathode were performed to further measure the performance of the as-prepared materials. The representative voltage profiles at different C rates are shown in Figure 8a. All of them are the second cycle curves after the C rate is changed from one to another (as shown in Figure 8c), and exhibit one major plateau for charging processes and two major plateaus for discharging processes, consistent with one major oxidation peak and two major reduction peaks observed during the anodic and cathodic scans of the CV test, respectively.

It is noted that the discharge capacities are extremely high. Specifically, as shown in Figure 8b, an initial discharge capacity as high as 1,029 mA h/g was obtained at the 0.2 C rate ($1C = 1166 \text{ mA/g}$). This specific capacity is 88% of the theoretical (1,166 mA h/g), indicating high utilization of Li_2S in the cathode. This high specific capacity demonstrates an excellent lithium uptake during lithiation in the cathode. In fact, 1,029 mA h/g is higher than *all* of the specific capacities of the encapsulated Li_2S reported by other researchers.^{6, 27-29} We attribute the ultrahigh high specific capacity to the superior core-shell structure which greatly enhance the utilization of Li_2S in the cathode, and further hypothesize that the $\text{Li}_2\text{S}/\text{C}$ composite core may play a role in attaining such a high initial specific capacity by providing some conductive networks within the Li_2S core to allow for most of the Li_2S to participate in electrochemical reactions.

The capacity retention of the coated Li_2S cathode is also very good. With prolonged cycles, the coin cell exhibits good capacity retention with around 650 mA h/g after 100 cycles at the 0.2 C rate. It should be pointed out that the capacity values achieved in this work are all based on the Li_2S active mass in the cathode. The quantity of the Li_2S in the carbon coated

Li₂S is estimated via weight measurement before and after carbonization of pyrrole, and found to be 72 wt%. The high Li₂S loading in the carbon coated Li₂S allows such carbon coated Li₂S cathodes to be coupled with lithium free anodes, circumventing the safety issues associated with the use of metallic Li anodes. Finally, as shown in Figure 8b, the Coulombic efficiency was not high initially, but gradually approached 98% after 100 cycles.

To further evaluate the electrode kinetics and stability of the core-shell structure, the coin cell was subject to cycling at different C-rates (Figure 8c). As indicated in the rate capability plot, when the rate was increased from 0.2 C to 0.5 C, the capacity decreased from 851 to 805 mA h/g. The capacity decreased again from 734 to 665 mA h/g when the rate increased from 0.5 C to 1 C. It is important to note that the battery still delivered a high capacity of 526 mA h/g even at the 2 C rate. After 40 cycles with different rates, the C rate was switched back to 0.2 C and the capacity was recovered to 758 mA h/g that is slightly higher than the capacity displayed by the cell if the cell is subject to 40 cycles at the 0.2 C rate continuously. These results illustrate the possibilities of fast kinetic reactions and the highly robust ability of our materials.

It should be mentioned that there is difference in the first charge voltage profile between the uncoated and carbon coated cells although the first activation charge is a transient process. As shown in Supplementary Information (Figure S1), both types of cells exhibit an initial potential hump at the early stage of the activation charging curve. This potential hump has been attributed to the energy barrier for nucleation of polysulfides.³⁹ Furthermore, the height of the potential hump is found to be associated with the thermodynamic barrier for nucleation as well as the kinetic factors, particularly the charge transfer overpotential associated with the formation of polysulfides.³⁹ In general, the carbon-coated cells have a lower potential barrier for nucleation than most of the uncoated cells, indicating the benefit of the nitrogen-doped carbon coating in reducing the charge transfer overpotential and facilitating the nucleation process. Furthermore, the carbon coated cells exhibit a long flat plateau after the initial potential hump. This long flat plateau is related to conversion of Li₂S to lower-order

polysulfides, then to higher-order polysulfides, and finally to elemental sulfur.³⁹ In contrast, the uncoated cells not only have higher potential barriers in most cases, but also exhibit a variety of different behaviors after the initial potential hump (Figure S1). We ascribe these different behaviors of the uncoated cells to the statistically random processes of ball milling of Li_2S with ~ 4.5 vol% CB and subsequent mixing of CB with the ball milled Li_2S during cathode fabrication. More discussions on the variation in the first charge behavior of the uncoated cells can be found in Supplementary Information.

To directly determine the enhanced capacity due to the nitrogen-doped carbon shell, comparisons in the electrochemical performance between the ball milled and coated electrodes were also investigated at 0.5 C. As shown in Figure 9, the cell with the carbon coated Li_2S electrode yielded an initial capacity of more than 850 mA h/g and retained 518 mA h/g even after 100 cycles at 0.5 C, while the battery with ball milled Li_2S cathodes delivered very low capacities. Compared to the uncoated Li_2S cathode, the carbon coated Li_2S electrode achieves much enhanced capacity, indicating that the carbon coating has increased the utilization of Li_2S in the cathode. However, Figure 9 also shows that the two cells have a very similar capacity fading rate, indicating that the carbon coating synthesized in this study is not very effective in reducing the dissolution and out-diffusion of high-order polysulfides. Therefore, the quality of the carbon coating needs to be improved in the future to enhance the capacity retention. Finally, it should be pointed out that the phenomenon of the similar capacity fading rate may not mean that the carbon coating has no effect on dissolution of polysulfides *at all*. The discussion on the possible effect of the carbon coating is provided in Supplementary Information.

Conclusions

In summary, we have established a facile method to prepare the $\text{Li}_2\text{S}/\text{C}$ composite particles encapsulated by nitrogen-doped carbon shells. Such an engineered $\text{Li}_2\text{S}-\text{C}$ structure proves to be excellent in achieving the extremely high initial discharge specific capacity, which is

higher than any previously reported values. Cells with this carbon-encapsulated Li_2S also exhibit good capacity retention. The excellent properties observed are attributed to the nitrogen-doped carbon shell which enhances both electronic and ionic conductivities, thereby greatly enhancing the utilization of Li_2S in the cathode. The $\text{Li}_2\text{S}/\text{C}$ composite core may also play a role in attaining the high discharge capacity. With a high mass ratio (72%) of active materials, the carbon coated Li_2S can be coupled with lithium free anodes, circumventing the safety issues associated with metallic lithium. Furthermore, the results and characterizations provided here enable better understanding of Li_2S cathodes and offer a way to design better electrodes in the future.

Acknowledgements – The use of the Center for Nanoscale Materials was supported by the U. S. Department of Energy, Office of Science, Office of Basic Energy Sciences, under Contract No. DE-AC02-06CH11357. The authors also would like to thank Jose Orozco for training of multiply instruments at IIT, Dr. Nancy L. Dietz Rago for FESEM training at ANL, and Dr. Xiao-min Lin at ANL for offering us the Gatan vacuum transfer holder for EFTEM measurement.

References

1. P. G. Bruce, S. A. Freunberger, L. J. Hardwick and J.-M. Tarascon, *Nat. Mater.*, 2012, **11**, 19.
2. Y. G. Guo, J. S. Hu and L. J. Wan, *Adv. Mater.*, 2008, **20**, 2878.
3. M. R. Palacín, *Chem. Soc. Rev.*, 2009, **38**, 2565.
4. B. Scrosati, *Chem. Rec.*, 2005, **5**, 286.
5. L. Chen and L. L. Shaw, *J. Power Sources*, 2014, **267**, 770.
6. C. Nan, Z. Lin, H. Liao, M. K. Song, Y. Li and E. J. Cairns, *J. Am. Chem. Soc.*, 2014, **136**, 4659.
7. K. Cai, M. K. Song, E. J. Cairns and Y. Zhang, *Nano Lett.*, 2012, **12**, 6474.
8. Y. Fu, Y.-S. Su and A. Manthiram, *Adv. Energy Mater.*, 2014, **4**, 1300655.
9. K. Han, J. Shen, C. M. Hayner, H. Ye, M. C. Kung and H. H. Kung, *J. Power Sources*, 2014, **251**, 331.
10. J. Hassoun and B. Scrosati, *Angew. Chem. Int. Ed. Engl.*, 2010, **49**, 2371.
11. W. Wei, J. Wang, L. Zhou, J. Yang, B. Schumann and Y. Nuli, *Electrochem. Commun.*, 2011, **13**, 399.
12. L. Yin, J. Wang, F. Lin, J. Yang and Y. Nuli, *Energy Environ. Sci.*, 2012, **5**, 6966.
13. S. Chen, X. Huang, H. Liu, B. Sun, W. Yeoh, K. Li, J. Zhang and G. Wang, *Adv. Energy Mater.*, 2014, **4**, 1301761.
14. G. Zheng, Y. Yang, J. J. Cha, S. S. Hong and Y. Cui, *Nano Lett.*, 2011, **11**, 4462.
15. S.-H. Chung and A. Manthiram, *Electrochem. Commun.*, 2014, **38**, 91.

16. L. F. Nazar, M. Cuisinier and Q. Pang, *MRS Bulletin*, 2014, **39**, 436.
17. B. Zhang, X. Qin, G. R. Li and X. P. Gao, *Energy Environ. Sci*, 2010, **3**, 1531.
18. C. Liang, N. J. Dudney and J. Y. Howe, *Chem. Mater.*, 2009, **21**, 4724.
19. H. S. Ryu, J. W. Park, J. Park, J.-P. Ahn, K.-W. Kim, J.-H. Ahn, T.-H. Nam, G. Wang and H.-J. Ahn, *J. Mater. Chem. A*, 2013, **1**, 1573.
20. X. Ji, K. T. Lee and L. F. Nazar, *Nat. Mater.*, 2009, **8**, 500.
21. L. Xiao, Y. Cao, J. Xiao, B. Schwenzer, M. H. Engelhard, L. V. Saraf, Z. Nie, G. J. Exarhos and J. Liu, *Adv. Mater.*, 2012, **24**, 1176.
22. G. Zheng, Q. Zhang, J. J. Cha, Y. Yang, W. Li, Z. W. Seh and Y. Cui, *Nano Lett.*, 2013, **13**, 1265.
23. H. Wang, Y. Yang, Y. Liang, J. T. Robinson, Y. Li, A. Jackson, Y. Cui and H. Dai, *Nano Lett.*, 2011, **11**, 2644.
24. X. Ji, S. Evers, R. Black and L. F. Nazar, *Nat. Commun.*, 2011, **2**, 325.
25. Z. Lin, Z. Liu, N. J. Dudney and C. Liang, *ACS Nano*, 2013, **7**, 2829.
26. S. Zheng, Y. Chen, Y. Xu, F. Yi, Y. Zhu, Y. Liu, J. Yang and C. Wang, *ACS Nano*, 2013, **7**, 10995.
27. Z. W. Seh, H. Wang, P.-C. Hsu, Q. Zhang, W. Li, G. Zheng, H. Yao and Y. Cui, *Energy Environ. Sci*, 2014, **7**, 672.
28. F. Wu, H. Kim, A. Magasinski, J. T. Lee, H.-T. Lin and G. Yushin, *Adv. Energy Mater.*, 2014, **4**, 1400196.
29. S. Jeong, D. Bresser, D. Buchholz, M. Winter and S. Passerini, *J. Power Sources*, 2013, **235**, 220.
30. R.-M. Ren, Z.-G. Yang and L. Shaw, *J. Mater. Sci.*, 2000, **35**, 6015.
31. Z.-G. Yang, R.-M. Ren and L. Shaw, *J. Am. Ceram. Soc.*, 2000, **83**, 1897.
32. R.-M. Ren, Z.-G. Yang and L. Shaw, *J. Am. Ceram. Soc.*, 2002, **85**, 819.
33. L. Shaw, M. Zawrah, J. Villegas, H. Luo and D. Miracle, *Metall. Mater. Trans.*, 2003, **34A**, 159.
34. C. Gong, Y.-J. Bai, Y.-X. Qi, N. Lun and J. Feng, *Electrochim. Acta*, 2013, **90**, 119.
35. J. Song, T. Xu, M. L. Gordin, P. Zhu, D. Lv, Y.-B. Jiang, Y. Chen, Y. Duan and D. Wang, *Adv. Funct. Mater.*, 2014, **24**, 1243.
36. L. Qie, W. M. Chen, Z. H. Wang, Q. G. Shao, X. Li, L. X. Yuan, X. L. Hu, W. X. Zhang and Y. H. Huang, *Adv. Mater.*, 2012, **24**, 2047.
37. L. Zhao, Y. S. Hu, H. Li, Z. Wang and L. Chen, *Adv. Mater.*, 2011, **23**, 1385.
38. Y. Shao, S. Zhang, M. H. Engelhard, G. Li, G. Shao, Y. Wang, J. Liu, I. A. Aksay and Y. Lin, *J. Mater. Chem.*, 2010, **20**, 7491.
39. Y. Yang, G. Zheng, S. Misra, J. Nelson, M. F. Toney and Y. Cui, *J. Am. Chem. Soc.*, 2012, **134**, 15387.

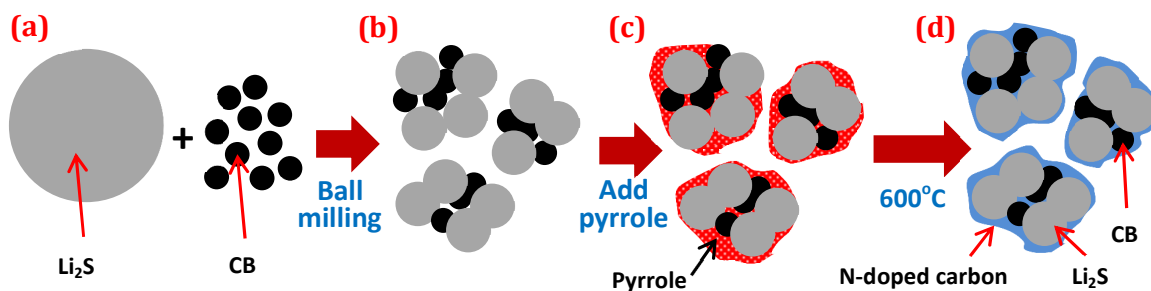


Figure 1. Schematic of the approach for synthesizing the $\text{Li}_2\text{S}/\text{C}$ composite particles encapsulated by a nitrogen-doped carbon shell: (a) mixing Li_2S with carbon black (CB), (b) the $\text{Li}_2\text{S}/\text{C}$ composite particles produced from high-energy ball milling, (c) mixing the composite particles with pyrrole, and (d) the $\text{Li}_2\text{S}/\text{C}$ composite particles encapsulated by a nitrogen-doped carbon shell.

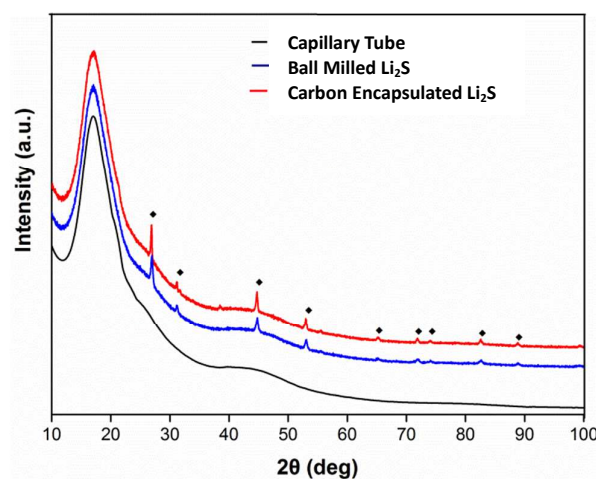


Figure 2. X-ray diffraction patterns of capillary tube, ball milled Li_2S and carbon encapsulated Li_2S . The black diamonds indicate the peaks of Li_2S (JCPDS Card No. 26-1188).

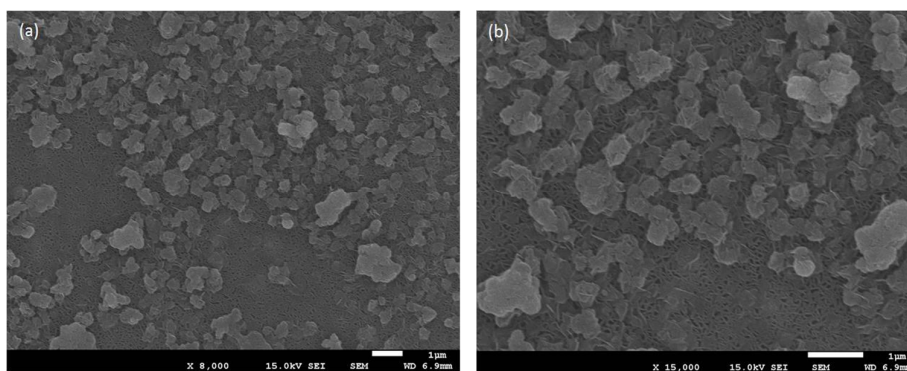


Figure 3. FESEM images of the carbon coated Li_2S : (a) Magnification $\times 8,000$, and (b) Magnification $\times 15,000$. The scale bar in both (a) and (b) corresponds to $1 \mu\text{m}$.

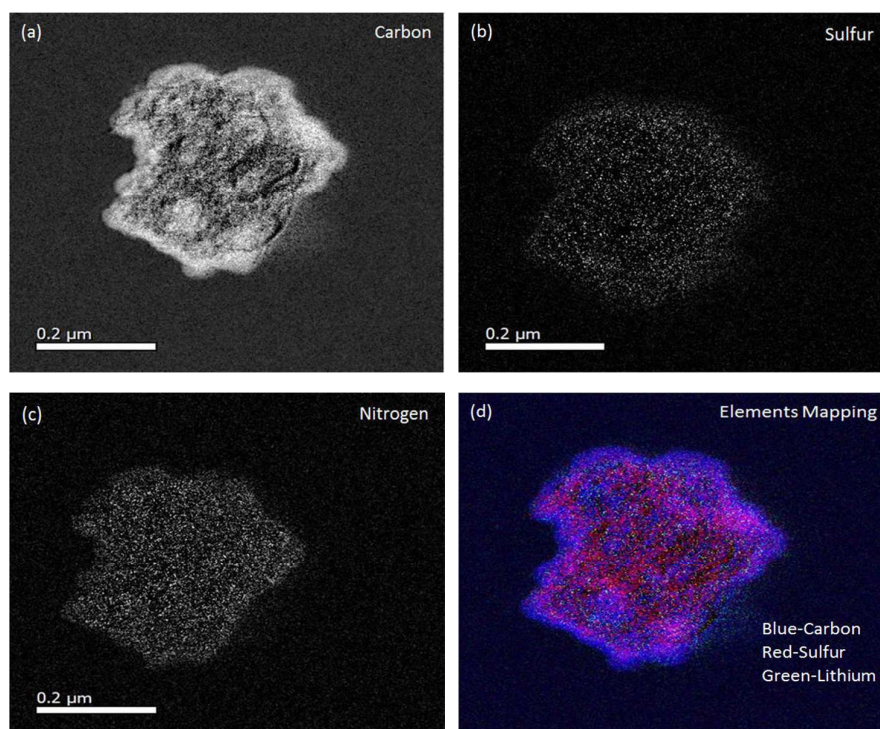


Figure 4. EFTEM elemental mapping of the carbon coated Li_2S : (a) carbon, (b) sulfur, (c) nitrogen, and (d) multi-element mapping (keys: blue-carbon, red-sulfur, and green-lithium).

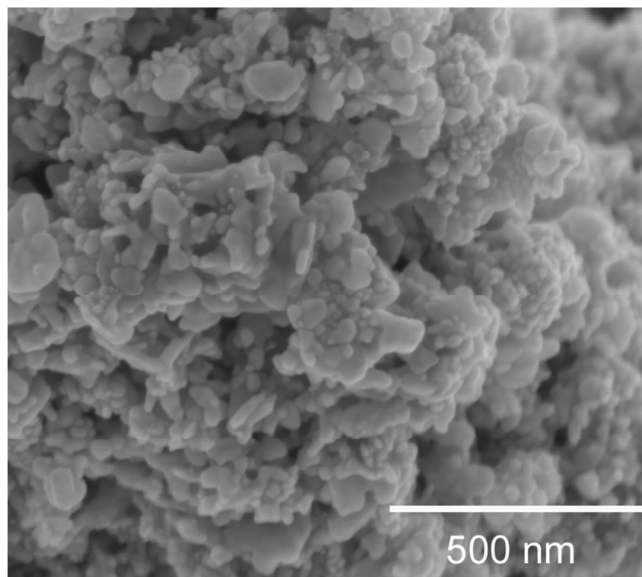


Figure 5. SEM image of the carbon black used with most particles in the range of 20 to 50 nm.

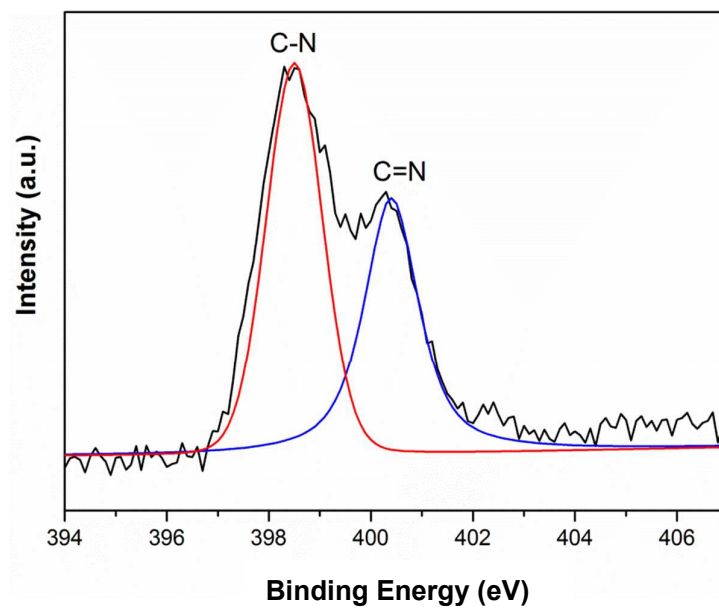


Figure 6. XPS spectra of N1s of the carbon coated Li₂S.

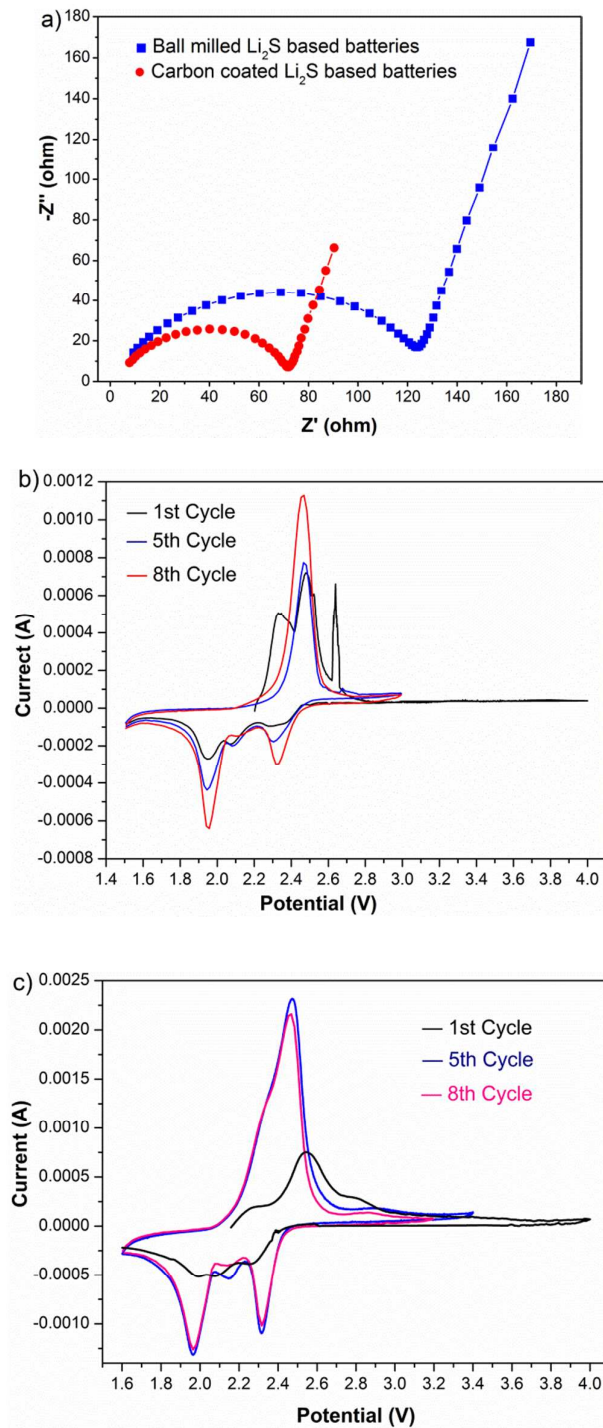


Figure 7. (a) EIS plots of Li_2S based batteries; (b) CV of the ball milled Li_2S -based cell at a potential sweep rate of 0.025 mV s^{-1} with an initial cutoff charge voltage of 4 V; and (c) CV of the carbon coated Li_2S -based cell at a potential sweep rate of 0.025 mV s^{-1} between 1.6 and 3.4 V, including an initial potential sweeping to 4 V.

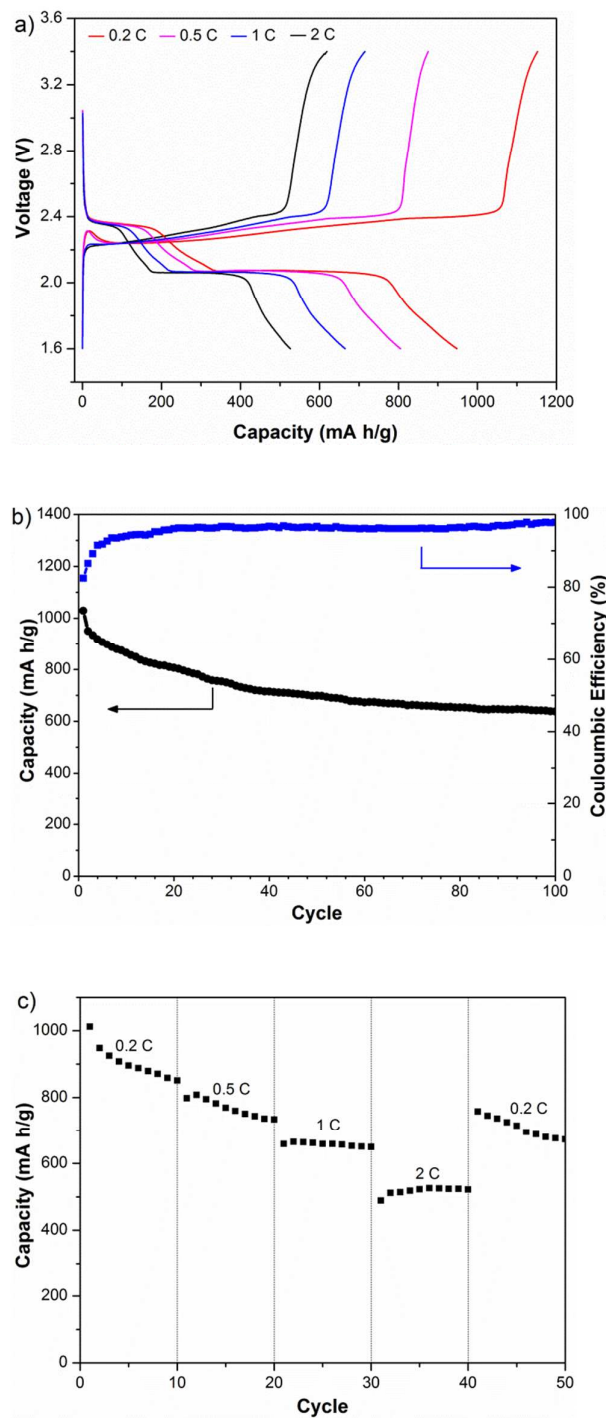


Figure 8. Electrochemical properties of the carbon coated Li_2S cells: (a) voltage profiles of the 2nd cycle at different C rates. 10 charge/discharge cycles were conducted at each C rate sequentially; (b) cycling performance and Coulombic efficiency at 0.2 C; and (c) specific capacity at different C rates and cycle numbers. The capacity values achieved in this work are based on the Li_2S active mass.

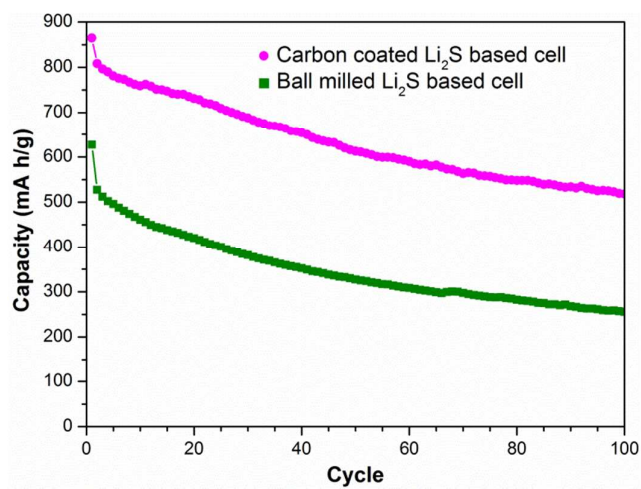


Figure 9. Cycling performances of the carbon coated Li₂S cell vs the ball milled Li₂S cell at the 0.5 C rate.

Li₂S Encapsulated by Nitrogen-Doped Carbon for Lithium Sulfur Batteries

Lin Chen ^{a,b}, Yuzi Liu ^c, Maziar Ashuri ^{a,b}, Caihong Liu ^{a,b} and Leon L. Shaw ^{a,b,*}

^a Wanger Institute for Sustainable Energy Research

^b Department of Mechanical, Materials and Aerospace Engineering
Illinois Institute of Technology, Illinois, USA

^c Center for Nanoscale Materials

Argonne National Laboratory, Illinois, USA

Supplementary Information

1. On the First Charge Voltage Profile

There is difference in the first charge voltage profile between the uncoated and carbon coated cells although the first activation charge is a transient process. As shown in Figure S1, both types of cells exhibit an initial potential hump at the early stage of the activation charging curve. This potential hump has been attributed to the energy barrier for nucleation of polysulfides.^{R1} Furthermore, the height of the potential hump is found to be associated with the thermodynamic barrier for nucleation as well as the kinetic factors, particularly the charge transfer overpotential associated with the formation of polysulfides.^{R1} The long flat plateau (Figure S1(b)) after the initial potential hump is related to conversion of Li₂S to lower-order polysulfides, then to higher-order polysulfides, and finally to elemental sulfur.^{R1} We note that the carbon-coated cell has a lower potential barrier for nucleation than most of the uncoated cells (as shown in Figure S1(a)), indicating the benefit of the nitrogen-doped carbon coating in reducing the charge transfer overpotential. In contrast, the uncoated cells not only have higher potential barriers in most cases, but also exhibit several different behaviors after the initial potential hump. These different behaviors include a long flat plateau (Figure S1(b)) and a long process with a gradual increase in the voltage (Figure S1(a)).

We ascribe the different charge behaviors of the uncoated cells to the statistically random processes of ball milling of Li₂S with ~4.5 vol% CB and subsequent mixing of CB with the ball milled Li₂S during cathode fabrication. As schematically shown in Figure 1b (see the article), most of the 4.5vol% CB will be embedded inside Li₂S particles during ball milling, but some may expose to the surface of Li₂S particles. We hypothesize that when many of the CB particles

added during cathode fabrication are in contact with those CB embedded in Li_2S particles but with exposure to the surface, the nucleation of polysulfides will be easy and the charge transfer overpotential will be low. As a result, the activation voltage profile of Figure S1(b) appears. However, if many of the CB particles added during cathode fabrication are in contact with the surface Li_2S particles directly, then the energy barrier for nucleation of polysulfides will be high and the charge transfer overpotential will be large. As a result, the activation curve of Figure S1(a) appears. Because of the random nature of the mixing and ball milling processes, the uncoated cells sometime display the first charge behavior of Figure S1(b), while in most cases the uncoated cells exhibit the first charge behavior of Figure S1(a).

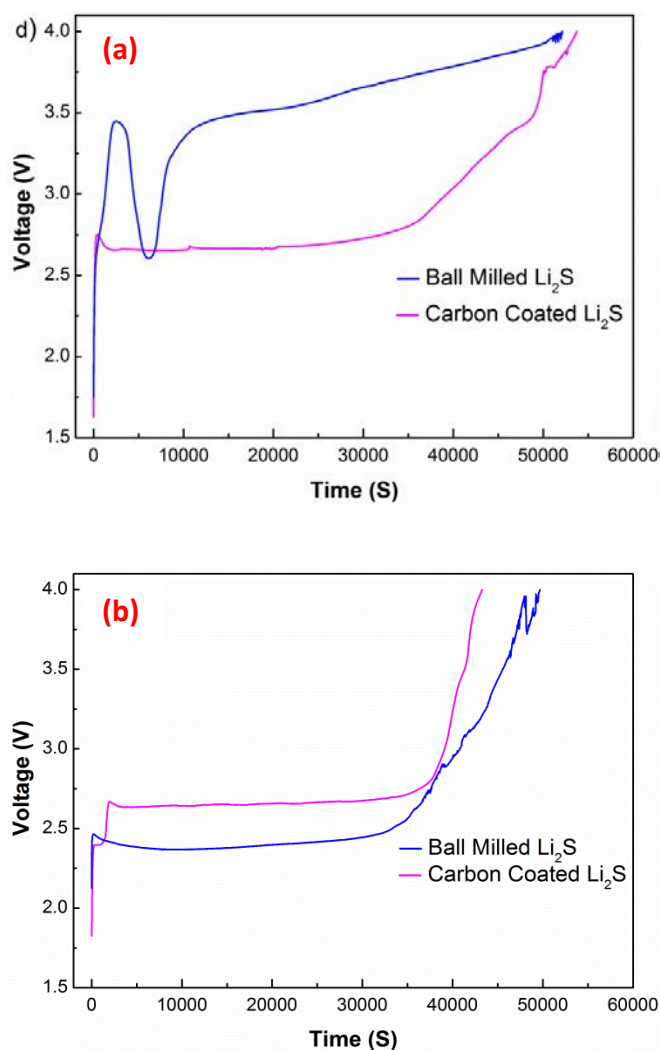


Figure S1. Voltage profiles of the first galvanostatic charge of ball milled Li_2S and carbon coated Li_2S cells as indicated with a C/20 rate. (a) and (b) show that ball milled Li_2S cells display two significantly different voltage profiles, whereas carbon coated Li_2S cells exhibit much consistent voltage profiles.

It is important to stress that the ball-milling embedded CB with exposure to the surface of Li_2S particles is more effective in reducing the charge transfer overpotential and making nucleation of polysulfides easier than the CB added during cathode fabrication because the contact between Li_2S and the embedded CB is intimate (due to compression during high-energy ball milling). In contrast, the contact between the CB added during cathode fabrication and the surface of Li_2S particles is relatively loose and may have a PVDF thin film between CB and Li_2S . This makes the CB added during cathode fabrication less effective in reducing the charge transfer overpotential associated with the formation of polysulfides. In addition, the gradually increased voltage profiles of Figure S1(a) after the initial potential drop suggest the presence of significant energy barriers for repeated nucleation of polysulfides and/or high charge transfer overpotential associated with the formation of polysulfides. This phenomenon is different from the carbon coated cells shown in Figure S1 and the observations reported in an earlier study.^{R1} Additional studies are needed in the future to understand this unusual phenomenon.

The carbon coated cells, in sharp contrast, display much more consistent behavior, i.e., a lower initial potential hump followed by a long flat plateau, as shown in Figure S1(a) and (b). This more consistent behavior is due to the presence of a nitrogen-doped carbon coating on the surface of *all* Li_2S particles, as schematically shown in Figure 1d. Clearly, this coating not only increases the utilization of Li_2S in the cathode (Figure 8), but also makes nucleation of polysulfides easier for all Li_2S particles and reduces the associated charge transfer overpotential substantially (Figure S1). Finally, it is worthy of mentioning that the carbon coated cells always display higher specific capacities than the uncoated cells regardless of their first charge potential profiles. This is true even for the case of Figure S1(b) where the uncoated cell displays a lower energy barrier for the nucleation process than the carbon coated counterpart. In spite of its lower energy barrier for the nucleation process, the uncoated cell has a lower specific capacity because Figure S1 does not tell us what percentage of Li_2S has participated in redox reactions during charge/discharge cycles. It only tells us what cell voltage is needed to activate the cell.

2. Discussion of the Effect of the Carbon Coating on Capacity Retention

Although Figure 9 shows that the two cells have a very similar capacity fading rate, it may not mean that the carbon coating has no effect on dissolution of polysulfides *at all*, as explained below. In a previous study,^{R2} it has been shown that the capacity fading can be

reduced by adding soluble polysulfides to the electrolyte. Further, the higher concentration of the soluble polysulfides in the electrolyte, the lower capacity fading rate will be,^{R2} suggesting that a high concentration of the soluble polysulfides in the electrolyte can slow down the dissolution of soluble polysulfides into the electrolyte during charge/discharge cycles.

If there is significant dissolution of polysulfides in the first charge process for the uncoated cells, then the concentration of polysulfides in the electrolyte will be higher for the uncoated cells than that for the carbon coated cells. As a result, there will be a smaller driving force for polysulfide dissolution in the uncoated cells because of its higher concentration of polysulfides in the electrolyte. Since the carbon coated cells have a higher driving force for polysulfide dissolution (because of its lower polysulfide concentration in the electrolyte after the first charge process), it would display a faster capacity fading rate than the uncoated cells. However, we did not observe this trend, suggesting that the carbon coating has some effect on impeding polysulfide dissolution.

References:

R1: Y. Yang, G. Zheng, S. Misra, J. Nelson, M. F. Toney and Y. Cui, *J. Am. Chem. Soc.*, 2012, **134**, 15387.

R2: S. Chen, F. Dai, M. L. Gordin, and D. Wang, *RSC Adv.*, 2013, **3**, 3540.